

Finite-difference modeling of scalar-wave propagation in cracked media

Gerben B. van Baren*, Wim A. Mulder[†], and Gérard C. Herman*

ABSTRACT

We discuss a finite-difference modeling technique for the simplified case of scalar, two-dimensional wave propagation in a medium containing a large number of small-scale cracks. The cracks are characterized by an explicit (Neumann) boundary condition whereas the embedding medium can be heterogeneous. The boundaries of the cracks are not represented in the finite-difference mesh, but the cracks are incorporated as distributed point sources. This enables the use of grid cells that are considerably larger than the crack sizes. We compare our method to an accurate integral-equation solution for the case of a homogeneous embedding and conclude that the finite-difference technique is accurate and computationally fast.

INTRODUCTION

Modeling wave propagation in media containing inclusions smaller than the wavelength of the probing wave field is of considerable interest in several areas, for instance, in seismology and in nondestructive evaluation. In seismology, variations in the subsurface of the earth are present on many scales: from scales much larger than the typical seismic wavelength down to scales that are much smaller. Heterogeneities that are much smaller than the seismic wavelength cannot be distinguished individually using seismic waves, but nevertheless can have a significant effect on the amplitude and phase of the transmitted wave field. O'Doherty and Anstey (1971) demonstrated this in their classic paper for the case of plane-stratified subsurface models.

In the long-wavelength limit, a homogeneous embedding containing small-scale heterogeneities effectively behaves as a homogeneous medium in which small-scale heterogeneities manifest themselves through apparent anisotropy and/or attenuation and dispersion. Most methods concerning wave

propagation in media with embedded inclusions are based on this concept of an effective medium. An excellent overview is given by Hudson and Knopoff (1989).

Alternatively, methods have been developed that focus on the calculation of transmitted wave fields by solving a boundary-value problem. Many of these methods are limited to plane-stratified models [see, for instance, Burridge and Chang (1989), who studied pulse propagation through a one-dimensional multilayered medium]. For the case of a large number of cracks embedded in a homogeneous medium, integral-equation techniques have been developed by Muijres et al. (1998).

All methods referred to in the previous paragraphs are not applicable to the case of cracks in the direct vicinity of a boundary or embedded in a heterogeneous medium. Nevertheless, these situations might arise when studying, for instance, wave propagation through a cracked reservoir in a layered earth or when investigating the propagation of boundary waves in tunnel walls containing cracks. Finite-difference techniques are well suited for solving wave propagation problems in heterogeneous media. The presence of cracks in this type of methods is accounted for by incorporating explicit boundary conditions at the crack location (see, for instance, Coates and Schoenberg, 1995; Carcione, 1996). This implies that each crack boundary has to be incorporated in the finite-difference mesh, requiring a prohibitive amount of grid points in the case of a large number of small-scale cracks. In the present paper, we develop a finite-difference technique for the computation of wave propagation of scalar, two-dimensional (2-D) waves in a heterogeneous medium containing a large number of small-scale cracks. Instead of imposing explicit boundary conditions at the crack boundaries, our method accounts for the presence of the cracks by introducing secondary point sources, the strength of which is computed using perturbation theory. In order to represent the point sources properly on a coarse finite-difference grid, we use an asymptotic method based on the integral representation of the scattered wave field of a small crack. We restrict ourselves to the scattering of 2-D, scalar waves by many small-scale cracks,

Manuscript received by the Editor December 21, 1998; revised manuscript received May 30, 2000.

*Delft University of Technology, Faculty of Technical Mathematics and Computer Science, Mekelweg 4, 2628CD Delft, The Netherlands. E-mail: g.c.herman@math.tudelft.nl.

[†]Shell International Exploration and Production BV, Postbus 60, 2280AB Rijswijk, The Netherlands. E-mail: w.a.mulder@sieep.shell.com.

© 2001 Society of Exploration Geophysicists. All rights reserved.

characterized by a Neumann boundary condition. This problem arises both in the scattering of *SH*-waves in a solid containing stress-free cracks and in the scattering of pressure waves in a fluid medium containing rigid cracks. In principle, also the (much more realistic) full elastic problem can be treated in a similar way, although this extension is definitely not straightforward. It requires the asymptotic form of the elastic wavefield scattered by a small crack and the use of the elastic finite-difference operator to this field in order to find the appropriate distribution of the crack over the grid points. During the review period of the present paper, we also solved the 2-D elastic problem; this will be the subject of a forthcoming paper.

Another important assumption upon which our method is based is the fact that interaction between individual cracks is neglected. For higher crack densities, this assumption is no longer valid, and we indicate how the method can be extended in order to take higher order scattering processes into account. The latter, however, is by no means a trivial extension.

REPRESENTATION OF THE SCATTERED FIELD IN TERMS OF SECONDARY SOURCES

We consider scalar 2-D wave propagation in an inhomogeneous medium containing a large number of small-scale cracks characterized by the Neumann boundary condition. In this paper, we discuss the case of a fluid medium containing rigid cracks, and formulate the problem in terms of the pressure. An identical formulation would describe the 2-D propagation of *SH*-waves in a solid containing stress-free cracks if the pressure in our formulation is replaced by the cross-line horizontal component of the particle velocity. The velocity of the medium, c , is a function of the 2-D position vector, $\mathbf{x} = (x, z)$, whereas the density is assumed constant everywhere. The m th crack is denoted by D_m , and its center is located at $\mathbf{x}_m = (x_m, z_m)$. This is illustrated in Figure 1. The unit vector normal to the crack is given by $\mathbf{n}_m = (\cos \varphi_m, \sin \varphi_m)$. The rigid crack is characterized by the Neumann boundary condition for the acoustic pressure p , given by

$$\mathbf{n}_m \cdot \nabla p(\mathbf{x}, t) = 0 \quad \mathbf{x} \in D_m. \quad (1)$$

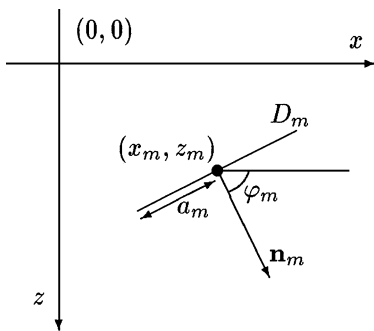


FIG. 1. Each crack is represented by a line segment D_m . It can be characterized by the position of its center, $\mathbf{x}_m = (x_m, z_m)$, its half-width a_m , and the angle φ_m with the horizontal. The z -coordinate indicates depth; the x -coordinate refers to the horizontal position. The unit vector normal to the crack is defined as $\mathbf{n}_m = (\cos \varphi_m, \sin \varphi_m)$.

In the region outside the cracks, the pressure satisfies the scalar wave equation

$$(c^{-2}\partial_{tt} - \Delta)p(\mathbf{x}, t) = s(\mathbf{x}, t) \quad \mathbf{x} \notin D_m, \quad (2)$$

where ∂_{tt} is the second-order time derivative, Δ denotes the 2-D Laplace operator, and $s(\mathbf{x}, t)$ is a source term generating the wave field. In principle, there are several ways of solving the boundary-value problem (1)–(2). For a homogeneous embedding (c constant), integral-equation methods can be used (Muijres et al., 1998). For the case of a heterogeneous embedding, however, these techniques may be impractical because they require a Green's function that is rather expensive to compute. Finite-difference techniques do not require the Green's function and are very well suited for the case of a heterogeneous embedding, but require many grid points in order to account for the explicit boundary condition (1) on the cracks. In the present paper, we reformulate the scattering problem in such a way that it can be incorporated in a finite-difference code without explicit modeling of the crack boundaries. This approach is especially designed for cracks that are much smaller than the typical finite-difference grid spacing.

The total pressure is first split into the incident field, p^{inc} , and scattered field, p^{sc} , in the following way:

$$p(\mathbf{x}, t) = p^{inc}(\mathbf{x}, t) + p^{sc}(\mathbf{x}, t). \quad (3)$$

By definition, the incident field satisfies the wave equation

$$(c^{-2}\partial_{tt} - \Delta)p^{inc}(\mathbf{x}, t) = s(\mathbf{x}, t) \quad \mathbf{x} \in \mathbb{R}^2 \quad (4)$$

(without any explicit boundary conditions on the cracks).

The scattered field then satisfies the source-free wave equation outside the cracks, i.e.,

$$(c^{-2}\partial_{tt} - \Delta)p^{sc}(\mathbf{x}, t) = 0 \quad \mathbf{x} \notin D_m, \quad (5)$$

whereas the presence of the cracks is accounted for by the explicit boundary condition

$$\mathbf{n}_m \cdot \nabla p^{sc}(\mathbf{x}, t) = -\mathbf{n}_m \cdot \nabla p^{inc}(\mathbf{x}, t), \quad \mathbf{x} \in D_m. \quad (6)$$

The scattered field can be expressed in terms of field quantities at the crack locations with the aid of a boundary-integral representation (Muijres et al., 1998). This representation has the simplest form after transforming all field quantities to the frequency domain by the temporal Fourier transform. In the frequency domain, this representation has the following form:

$$\hat{p}^{sc}(\mathbf{x}) = - \sum_m \int_{\mathbf{x}' \in D_m} \mathbf{n}_m \cdot \nabla \hat{p}^G(\mathbf{x}, \mathbf{x}') \hat{\phi}_m(\mathbf{x}') dS, \quad \mathbf{x} \notin D_m, \quad (7)$$

where $\hat{\cdot}$ denotes a Fourier-transformed quantity, $\hat{\phi}_m$ is the pressure jump across the m th crack, and \hat{p}^G denotes the Green's function of the embedding medium. For brevity, the frequency dependence of all quantities is omitted. The Green's function \hat{p}^G is defined as the solution of the Helmholtz equation for the embedding, given by:

$$(-\omega^2 c^{-2} - \Delta)\hat{p}^G(\mathbf{x}, t) = \delta(\mathbf{x} - \mathbf{x}'), \quad \mathbf{x} \in \mathbb{R}^2, \quad (8)$$

where $\delta(\mathbf{x} - \mathbf{x}')$ denotes a point source at position $\mathbf{x} = \mathbf{x}'$.

This study is restricted to small-scale cracks, i.e., the scale of the cracks is small compared to the scale on which the wave

field varies. If the cracks are small enough, we can neglect the variation of the Green's function during the integration over each crack and we can rewrite equation (7) as

$$\hat{p}^{sc}(\mathbf{x}) = - \sum_m \mathbf{n}_m \cdot \nabla \hat{p}^G(\mathbf{x}, \mathbf{x}_m) \int_{\mathbf{x}' \in D_m} \hat{\phi}_m(\mathbf{x}') dS, \quad \mathbf{x} \notin D_m, \quad (9)$$

which implies that each crack acts as a dipole point source for the scattered field. By retaining the jump function $\hat{\phi}_m$ under the integral, we can still properly account for the occurrence of singularities at the crack tips. When we compare equation (9) with equation (8), we conclude that the scattered field \hat{p}^{sc} can be interpreted as the solution of the following equation:

$$(-\omega^2 c^{-2} - \Delta) \hat{p}^{sc}(\mathbf{x}) = - \sum_m \mathbf{n}_m \cdot \nabla \delta(\mathbf{x} - \mathbf{x}_m) \times \int_{\mathbf{x}' \in D_m} \hat{\phi}_m(\mathbf{x}') dS, \quad \mathbf{x} \in \mathbb{R}^2, \quad (10)$$

where the explicit boundary conditions at the cracks are replaced by secondary point sources at the crack locations. Of course, in order to compute the secondary source strengths $\hat{\phi}_m$ at the cracks, the boundary conditions still have to be imposed. An integral-equation formulation for the source strengths can be obtained by taking the normal derivative of equation (7), letting the point of observation approach the cracks and applying the boundary condition (6). However, this approach is impractical for heterogeneous media because computation of the Green's function can be computationally very expensive. Therefore, we approach the problem in a different way by approximating the source strengths $\hat{\phi}_m$ with the aid of perturbation theory and using a finite-difference formulation for computing the solution of equation (10). Perturbation theory results in an approximate source strength (De Hoop, 1955a; Muijres et al., 1998)

$$\int_{\mathbf{x}' \in D_m} \hat{\phi}_m(\mathbf{x}') dS \cong \pi a_m^2 \hat{q}_m, \quad (11)$$

where

$$\hat{q}_m = \mathbf{n}_m \cdot \nabla \hat{p}^{inc}(\mathbf{x}_m) \quad (12)$$

and a_m is the half-width of the crack (Figure 1). This approximation is based upon the following assumptions:

- 1) Second- and higher-order scattering effects, i.e., the interactions between the different cracks, are neglected.
- 2) The crack size is small compared to the wavelength of the incident wave. This implies that the incident wave is considered to be locally plane at the location of the crack and that the source strength $\hat{\phi}_m$ can be approximated by the leading-order term in a perturbation series with $\omega a_m / c$ as small parameter (De Hoop, 1955a, b; see also Muijres et al., 1998).

The first assumption is the most restrictive one in our case. In principle, it can be relaxed by taking higher-order terms into account in the Neumann-series expansion of $\hat{\phi}_m$ (Muijres et al., 1998).

If we now combine equations (10) and (11) and transform the resulting equation back to the time domain, we obtain the

following wave equation for the scattered wave field:

$$(c^{-2} \partial_{tt} - \Delta) p^{sc}(\mathbf{x}, t) = - \sum_m \pi a_m^2 q_m(t) \mathbf{n}_m \cdot \nabla \delta(\mathbf{x} - \mathbf{x}_m) \quad \mathbf{x} \in \mathbb{R}^2, \quad (13)$$

with q_m the inverse Fourier transform of \hat{q}_m , which can be expressed in terms of the incident field by the relation

$$q_m(t) = \mathbf{n}_m \cdot \nabla p^{inc}(\mathbf{x}_m, t). \quad (14)$$

The scattering problem can be solved with the finite-difference method. First, the incident field is computed by solving Eq. (4) for the (heterogeneous) embedding without accounting for the presence of the cracks; second, the (first-order) scattered field is obtained by solving equation (13) with a similar technique. In this way, the problem of accounting for the explicit boundary conditions on many small cracks is avoided and replaced by the problem of accounting for the presence of many small point sources on a finite-difference grid. This is discussed in the next section. In order to find a good representation of the dipole point sources occurring on the right side of equation (13), we need a representation of the wave field in the direct vicinity of each crack. If we assume that the speed of sound in the direct vicinity of the m th crack is constant, we can express the scattered field p_m^{sc} from this single crack in the form

$$p_m^{sc}(\mathbf{x}, t) = -\pi a_m^2 \mathbf{n}_m \cdot \nabla \int_{\rho}^{\infty} d\tau \frac{q_m(t - \tau)}{2\pi \sqrt{\tau^2 - \rho^2}} \quad (\mathbf{x} \cong \mathbf{x}_m), \quad (15)$$

where $\rho(\mathbf{x}, \mathbf{x}_m) = |\mathbf{x} - \mathbf{x}_m|/c(\mathbf{x}_m)$ is the arrival time of waves from the center of the crack \mathbf{x}_m to the observation point \mathbf{x} . This equation is obtained by computing the inverse Fourier transform of the m th term of the summation on the right side of equation (7) and using the fact that the frequency-domain Green's function \hat{p}^G for a homogeneous embedding is given by

$$\hat{p}^G(\mathbf{x}, \mathbf{x}_m) = \frac{i}{4} H_0^{(1)}(\omega r_m(\mathbf{x})/c(\mathbf{x}_m)) \quad (\mathbf{x} \cong \mathbf{x}_m), \quad (16)$$

with r_m given by

$$r_m(\mathbf{x}) = |\mathbf{x} - \mathbf{x}_m|, \quad (17)$$

and where $H_0^{(1)}$ is the zeroth-order Hankel function of the first kind (see also Muijres et al., 1998). To account for the square-root singularity in equation (15), partial integration is used twice to obtain

$$p_m^{sc}(\mathbf{x}, t) = \frac{a_m^2 \mathbf{n}_m \cdot (\mathbf{x} - \mathbf{x}_m)}{2 r_m^2(\mathbf{x})} \int_{\rho}^{\infty} d\tau \partial_{tt} q_m(t - \tau) \sqrt{\tau^2 - \rho^2}. \quad (18)$$

Here, we have assumed $q_m(-\infty) = 0$, because of causality. Relation (18) shows an important characteristic of the scattered field in a 2-D geometry. The whole time history of $q_m(t)$ has to be taken into account in order to calculate $p_m^{sc}(\mathbf{x}, t)$. Because a 2-D point source can be interpreted as the projection of a three-dimensional (3-D) line source with infinite length, each point of the line source actually contributes to the scattered field, causing a long tail in time. This could represent a problem for the finite-difference technique, since the computation of the integral is rather time-consuming. We show in the next

section that this problem can be circumvented by using a series expansion for the Green's function.

FINITE-DIFFERENCE METHOD

In the previous section, the effect of each crack has been accounted for by the presence of a dipole point source with a strength determined by the half-width a_m and the incident field. Because point sources cannot be accurately represented in a finite difference scheme (in particular, if the position of the crack does not coincide with a grid point), subgrid modeling is used. This means that the effect of the crack has to be distributed over its surrounding grid points. These grid points together should produce the same scattered field as the crack.

The discrete counterpart of the wave equation can be obtained from equation (2) by approximating the partial derivatives by finite differences and taking the quantities $p(\mathbf{x}, t)$ and $s(\mathbf{x}, t)$ at a grid point \mathbf{x}_{ij} and discrete time t_n .

The scheme by Dablain (1986) is used for the temporal discretization of the wave operator. When choosing fourth-order accuracy in time, this scheme reads

$$B^h p_{i,j}^n \equiv \frac{p_{i,j}^{n+1} - 2p_{i,j}^n + p_{i,j}^{n-1}}{(c_{i,j} \Delta t)^2} - \Delta^h p_{i,j}^n - \frac{(c_{i,j} \Delta t)^2}{12} (\Delta^h)^2 p_{i,j}^n. \quad (19)$$

Here, B^h is the discrete wave operator, being the discretization of $B = c^{-2} \partial_{tt} - \Delta$, $c_{ij} = c(\mathbf{x}_{ij})$ and Δ^h is the discretization of the Laplace operator Δ . The time step is denoted by Δt . The second-order spatial derivative is approximated by an eighth-order scheme. For the discrete wave equation, we then obtain

$$\frac{p_{i,j}^{n+1} - 2p_{i,j}^n + p_{i,j}^{n-1}}{(c_{i,j} \Delta t)^2} - \left[\Delta^h + \frac{(c_{i,j} \Delta t)^2}{12} (\Delta^h)^2 \right] p_{i,j}^n = s_{i,j}^n. \quad (20)$$

In our scheme, this approach is followed both for computing the incident field p^{inc} with the aid of equation (4) and, subsequently, the scattered field p^{sc} from equation (13). In solving the latter equation, however, we have to represent a large number of dipole point sources in the finite-difference scheme.

To incorporate these point sources, several options can be considered:

- 1) The use of a dipole point source convolved with a Gaussian in space as a source term for the scattered field.
- 2) Replacement of the numerically computed scattered field from equation (20) without the source term by the analytically computed field from equation (18) in the neighborhood of the crack.
- 3) Derivation of the discrete source term from the analytically computed field [relation (18)] and the finite-difference operator.

The first option is the easiest to implement. For the finite difference simulation, 3–5 points per wavelength are required to keep the numerical errors sufficiently small. Therefore, a Gaussian with a width of a few wavelengths will not destroy too much of the accuracy of the scheme. The width cannot be too large, otherwise the higher frequencies will be removed; nor can it be too small, otherwise the singular character of the source term will have an adverse effect on the accuracy.

More accurate solutions are obtained by the second and third option. In the second approach, the solution of equation (20) is computed at every time step without using the source term. After a time step, the solution in the neighborhood of the crack, say a square region of 8×8 points around the crack, is replaced by the analytical solution of equation (18) evaluated at grid points. In this way, we obtain a simple implementation of a domain decomposition method with an analytical solution around the crack and a finite-difference solution elsewhere. This approach works fine for one crack but problems occur with multiple cracks. In that case, the scattered field contains contributions from several cracks and cannot be simply replaced by the response of just one crack. The summed result of all cracks has to be considered, making this approach viable but rather expensive.

We have considered the third option, based on the determination of the secondary point sources by applying the (discrete) wave operator to the scattered field [relation (18)]. In this method, the effect of the point source is distributed over its neighboring grid points. Since this distribution is done with the aid of the finite-difference operator, it is more accurate than the first option, where the operator is not used in distributing the point source by convolving it with a Gaussian. The discrete version of the wave equation $Bp = s$ can be denoted by $B^h p^h = s^h$. Let \tilde{I}^h be the restriction of the continuous representation of the operator to its discretized version. Likewise, the restriction of the continuous representation of the solution to the grid can be denoted by I^h . In the present case, this restriction operator amounts to sampling at the grid points. If I_h defines the injection, or interpolation, from the solution on the grid to the continuous representation, then we can write $B^h = \tilde{I}^h B I_h$. A discrete source term can be obtained by letting

$$s^h = \tilde{I}^h s = \tilde{I}^h B p \approx \tilde{I}^h B I_h I^h p = B^h I^h p.$$

The approximation made here is that $I_h I^h \approx I$, meaning that the continuous solution p can be represented on the grid with sufficient accuracy. If time step Δt and grid spacings Δx and Δz have been chosen properly with respect to the frequency content of the incident wave, this assumption is reasonable.

The discrete version of the scattered field p_m^{sc} due to the m th crack is given by $p_m^{sc}(\mathbf{x}_{i,j}, t_n)$, which is simply equation (18) evaluated at grid points $\mathbf{x}_{i,j}$ and times t_n . Note that this representation assumes that the velocity is constant in the direct vicinity of the crack ($\mathbf{x}_{i,j} \cong \mathbf{x}_m$). The integral is computed numerically using the trapezoid rule. To obtain $q_m^h(t_n)$ at the crack, eighth-order Lagrangian interpolation and differentiation polynomials are used. Its second time-derivative $(\partial_{tt} q_m)^h(\tau)$ is computed by a fourth-order Lagrangian differentiation polynomial. If we compute equation (18) at each time and in each grid point, and substitute the resulting values in equation (20), we obtain the source distribution at each time and in each grid point:

$$s_{i,j}^n = \frac{p_m^{sc}(\mathbf{x}_{i,j}, t_{n+1}) - 2p_m^{sc}(\mathbf{x}_{i,j}, t_n) + p_m^{sc}(\mathbf{x}_{i,j}, t_{n-1})}{(c_{i,j} \Delta t)^2} - \left[\Delta^h + \frac{(\mu_{i,j} \Delta s)^2}{12} (\Delta^h)^2 \right] p_m^{sc}(\mathbf{x}_{i,j}, t_n). \quad (21)$$

Here, we have used the same grid spacing in x and z , namely $\Delta s = \Delta x = \Delta z$. Furthermore, we have $\mu_{ij} = c_{ij} \Delta t / \Delta s$.

Because we are modeling a point source, we expect that the numerically constructed source distribution shows a local dominant behavior near the crack position. It therefore seems acceptable to compute the source distribution in a restricted area around the crack only. In that way, the number of points, in which equation (18) has to be computed, can be reduced. This is supported by Figure 2, where the numerically constructed source distribution of a horizontally oriented crack is plotted at the instant where the incident field has reached its maximum value at the crack location. Figure 2(a) shows the source distribution $s_{i,j}$ in the region near the crack, with a contour plot at the bottom. Figure 2(b) is a cross-section at $x = 0$. Although there are nonzero values away from the crack, it is highly dominated by the two peaks. Two factors influence the size of this region. If we choose it too small, information is cut off, resulting in larger errors. On the other hand, the more points we choose, the more computer memory and processing time are required. In the experiments, we have chosen this region to consist of 8×8 grid points. Outside this region, the source is assumed to be zero.

This method uses the integral representation, which is only valid in homogeneous media. Therefore, the grid points involved in the area around a crack have to be in a layer with (almost) constant velocity. In the case of multiple cracks, it does not matter if the areas of neighboring cracks overlap each other. Since the wave equation is linear, different sources can be added without any problems. If two cracks are close to the same grid point, we just take the sum of the two source values at that point.

The above method for representing small cracks has some computational drawbacks. Since we use the integral representation of the scattered field, we have to store the normal derivative of the incident field for each crack at all past times. This requires an enormous amount of memory in the case of several thousands of cracks. Furthermore, the processing time to compute equation (18) in all 64 grid points around each crack is significant.

To avoid these disadvantages, we have constructed an explicit source representation. First, we consider $\hat{B}^h \hat{p}_m^{sc}(\mathbf{x}, \omega)$ in

the space-frequency domain and approximate it by a truncated series expansion in $k_0 r_m$ of the scattered field, where k_0 is related to the angular frequency through the relation

$$k_0 = \frac{\omega}{c(\mathbf{x}_m)}, \quad (22)$$

and r_m is given by equation (17). Finally, the results are transformed back to the space-time domain.

For the counterpart of the discrete wave operator (19) in space-frequency domain, we obtain

$$\hat{B}^h = -k_0^2 + \frac{(\mu_{i,j} \Delta s)^2}{12} k_0^4 - \left[\Delta^h + \frac{(\mu_{i,j} \Delta s)^2}{12} (\Delta^h)^2 \right], \quad (23)$$

which is derived in Appendix A. The space-frequency counterpart of the scattered field due to the m th crack, \hat{p}_m^{sc} , follows from equation (15) as

$$\begin{aligned} \hat{p}_m^{sc}(\mathbf{x}, \omega) &= -\pi a_m^2 \mathbf{n}_m \cdot \nabla \frac{i}{4} H_0^{(1)}(\omega r_m(\mathbf{x})/c(\mathbf{x}_m)) \hat{q}_m(\omega) \\ &\quad (\mathbf{x} \cong \mathbf{x}_m) \\ &= \pi a_m^2 \frac{\mathbf{n}_m \cdot (\mathbf{x} - \mathbf{x}_m)}{r_m(\mathbf{x})} \frac{ik_0}{4} H_1^{(1)}(k_0 r_m(\mathbf{x})) \hat{q}_m(\omega). \end{aligned} \quad (24)$$

If we apply the space-frequency domain discrete wave operator to \hat{p}_m^{sc} of equation (24), $\hat{B}^h \hat{p}_m^{sc}$ can be written as

$$\begin{aligned} \hat{B}^h \hat{p}_m^{sc}(\mathbf{x}, \omega) &= \pi a_m^2 \left\{ \left(-k_0^2 + \frac{(\mu_{i,j} \Delta s)^2}{12} k_0^4 \right. \right. \\ &\quad \left. \left. - \left[\Delta^h + \frac{(\mu_{i,j} \Delta s)^2}{12} (\Delta^h)^2 \right] \right) \right. \\ &\quad \left. \times \left(\frac{\mathbf{n}_m \cdot (\mathbf{x} - \mathbf{x}_m)}{r_m} \frac{ik_0}{4} H_1^{(1)}(k_0 r_m) \right) \right\} \hat{q}_m(\omega), \end{aligned} \quad (25)$$

$$\hat{q}_m(\omega) = \mathbf{n}_m \cdot \nabla \hat{p}^{inc}(\mathbf{x}_m, \omega).$$

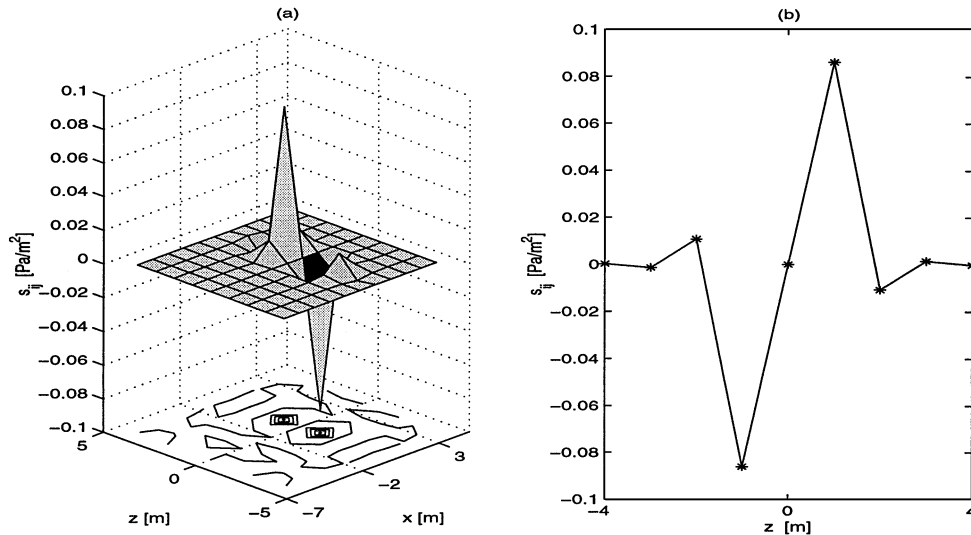


FIG. 2. Numerically constructed source distribution of a horizontally oriented crack as a function of x and z (a) and a vertical cross-section through the center of the crack (b). The source values are computed by applying the discrete wave operator to the numerically computed values of the scattered pressure in the grid points.

Using the series expansion of the Hankel function up to fourth order for small $k_0 r_m$, the part between the curly braces in equation (25) can be expressed as a polynomial in k_0 with coefficients depending only on \mathbf{x} and \mathbf{x}_m :

$$\hat{B}^h \hat{p}_m^{sc}(\mathbf{x}, \omega) \cong \pi a^2 [A_0(\mathbf{x}, \mathbf{x}_m) - k_0^2 A_2(\mathbf{x}, \mathbf{x}_m) + k_0^4 A_4(\mathbf{x}, \mathbf{x}_m)] \hat{q}_m(\omega), \quad (26)$$

where the coefficients A_0 , A_2 , and A_4 are given in Appendix B [equations (B.6)–(B.8)]. Approximation (26) is valid if the wavelength is large in comparison with the finite-difference grid spacing. The space-time counterpart of equation (26) is easily obtained, since the powers of k_0 are all transformed into time derivatives of $q_m(t)$. Finally, we have to combine the contributions of all cracks, and we find the following source term:

$$s(\mathbf{x}, t) = \sum_m \pi a_m^2 \left(A_0(\mathbf{x}, \mathbf{x}_m) q_m(t) + A_2(\mathbf{x}, \mathbf{x}_m) \frac{1}{c^2} \partial_{tt} q_m(t) + A_4(\mathbf{x}, \mathbf{x}_m) \frac{1}{c^4} \partial_{tttt} q_m(t) \right). \quad (27)$$

After discretization, we arrive at

$$s_{i,j}^n = \sum_m \pi a_m^2 \left(A_0(\mathbf{x}_{i,j}, \mathbf{x}_m) q_m^h(t_n) + A_2(\mathbf{x}_{i,j}, \mathbf{x}_m) \frac{1}{c_{i,j}^2} (\partial_{tt} q_m)^h(t_n) + A_4(\mathbf{x}_{i,j}, \mathbf{x}_m) \frac{1}{c_{i,j}^4} (\partial_{tttt} q_m)^h(t_n) \right), \quad (28)$$

where the time derivatives can be determined by finite differences.

Because the coefficients A_0 , A_2 , and A_4 rapidly decrease in size with increasing distance from each crack, the source distribution can be limited to a small region around the crack. Outside this region, the coefficients are assumed to be zero. In the experiments, this region consists of 8×8 points. Because the coefficients A_0 , A_2 , and A_4 do not depend on time, they can be computed only once and stored in a grid belonging to a specific crack. The storage space, necessary for storing the coefficients, is 3×64 times the number of cracks. The main additional computational effort involves the computation of the time derivatives of $q_m^h(t)$ and the fact that the incident and scattered fields have to be computed and stored separately. This implies that the CPU time required for the cracked medium is about 2–3 times the CPU time required for computing the field in the absence of cracks. Also, memory requirements for storing the two fields have doubled with an additional storage requirement for storing the crack scattering coefficients (depending on the number of cracks, see above). The method, obtained in this way, enables us to model the scattering of cracks in an efficient and accurate way. It can easily handle several thousand cracks.

So far, we have described only first-order scattering. The effect of multiple scattering arises in the case of more than one crack. This effect is of increasing importance with increasing crack density. For example, second-order scattering of a crack can be computed by taking the first-order scattered field as incident field, excluding the scattered field of that specific crack (Muijres et al., 1998).

In the finite-difference scheme, second-order scattering in principle can be implemented by using the first-order scattered field in a source term for another wave equation describing the second-order scattered field. Care should be taken that the cracks do not feed on their own scattered field, that is, the scattered field of a particular crack should be removed from the scattered field that drives the source term for the same crack. However, when attempting to compute multiple scattering, we encountered severe accuracy problems. These might be due to the singular character of the scattered field close to the crack and to the high number of temporal derivatives of the wavefield [see equation (28)] that need to be taken but may not exist.

We have also tried a very simple approach. Instead of splitting the pressure field in incident and scattered terms, only one wave equation for the total pressure with a source term driven by the same total pressure was considered. This led to severe instabilities, caused by a feedback loop at each crack. Although the scattered field should move away from a given crack, numerical errors will move back, causing the source term to be fed by errors in its own scattered field rather than the incident field. The application of the source term in a separate equation for the first-order scattered field avoids this instability.

VALIDATION OF THE METHOD

In order to validate our finite-difference (FD) method, we consider the third option, with the cracks distributed over the grid points as indicated in equation (28) and compare it, for the case of a homogeneous embedding, with a boundary integral equation (BIE) method described by Muijres et al. (1998). The BIE method is not based on the perturbation approach as the FD approximation used in our method, and is not limited to first-order scattering only.

We consider a geometry with 3000 horizontally aligned cracks in a rectangular region of $500 \text{ m} \times 200 \text{ m}$, each crack with half-width $a_m = 1 \text{ m}$. Their positions are random. The wave field is computed at 50 receivers, placed at $z = 0 \text{ m}$, 20 m apart in the horizontal direction. As incident field, we have taken a plane wave with a Ricker wavelet source wave form (dominant frequency: 45 Hz). The incident wave is propagating vertically downward (i.e., in a direction normal to the orientation of the cracks). The incident wave has its maximum value at $t = 0 \text{ s}$ and $z = 0 \text{ m}$. The sound speed in the homogeneous background is $c = 2500 \text{ m/s}$. The results are shown in Figure 3; a more detailed comparison is made in Figure 4. The results are very similar. Apparently, multiple-scattering effects are negligible for this case. If the crack density increases, however, these higher-order effects can be more pronounced (Muijres et al., 1998).

MODEL STUDY FOR A CROSS-WELL GEOMETRY

To illustrate the versatility of our method, we have simulated a crosswell experiment. We consider a low-velocity layer, containing cracks, between two high-velocity layers. The geometry is shown in Figure 5. A seismic source, situated in the low-velocity layer, generates the wave field; the wave field is computed at the receivers, positioned in a vertical borehole. The receivers are located at $x = 1000 \text{ m}$. Their depth-coordinate ranges from $z = 1000$ to 2000 m , the vertical spacing equals 20 m . The low-velocity layer is positioned between $z = 1300$ and 1700 m . When the source is located in the low-velocity layer in between the two high-velocity layers, most energy emitted by

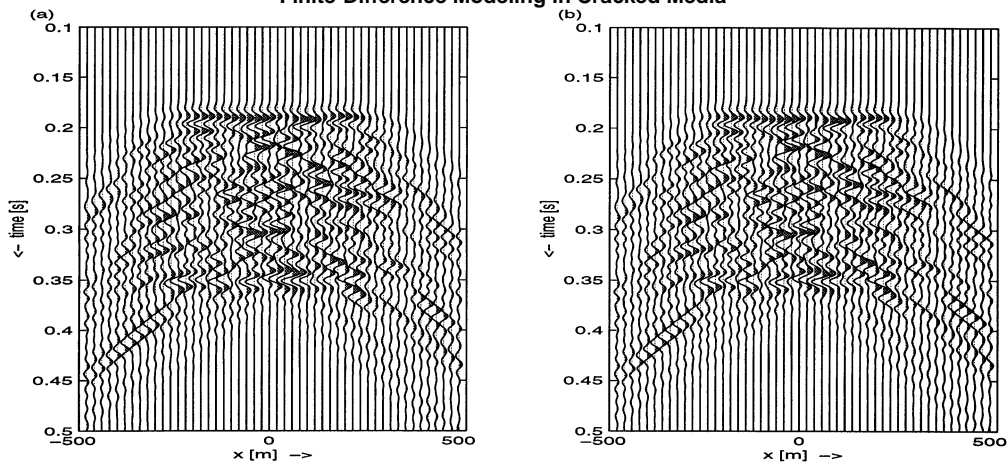


FIG. 3. Comparison of the scattered fields of the FD method (a) and BIE method (b). An incident plane wave is scattered from a region with 3000 horizontally oriented cracks, embedded in a homogeneous medium with sound speed $c = 2500$ m/s. The scattered wave field is shown at $z = 0$ m.

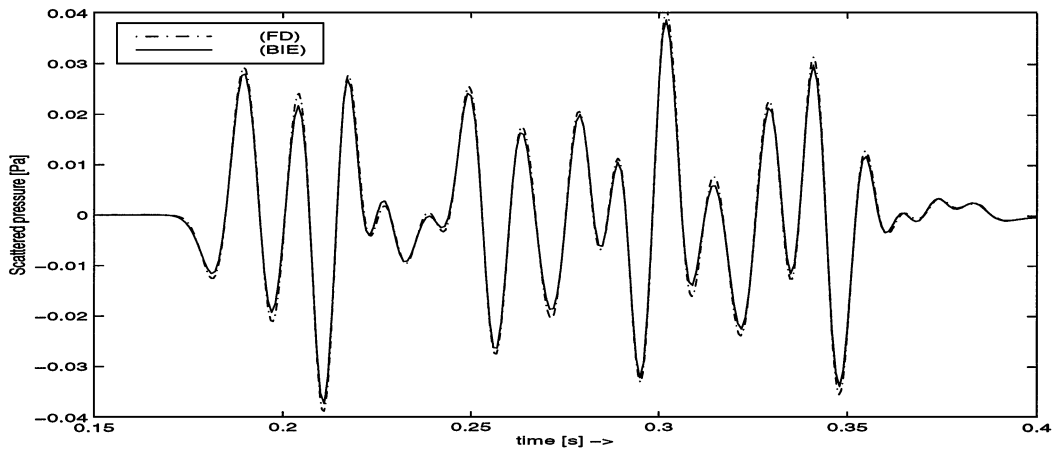


FIG. 4. More detailed comparison of the wave fields at $(x, z) = (0, 0)$ of Figure 3 computed with the FD and BIE methods.

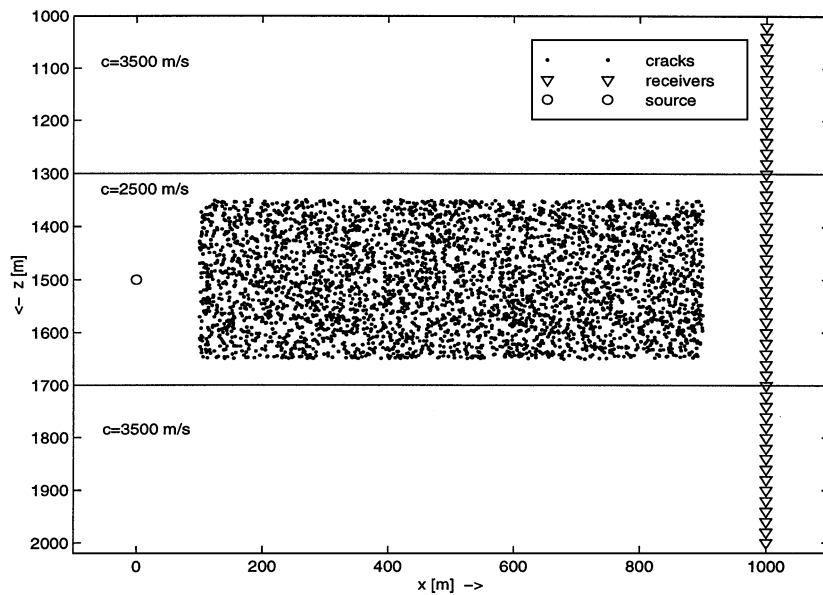


FIG. 5. Geometry of the crosswell simulation. A low-velocity layer ($c = 2500$ m/s), containing 4000 randomly positioned cracks, is embedded in two high-velocity layers ($c = 3500$ m/s). The seismic source is located in the low-velocity layer (on the left side), whereas the receivers are positioned in a vertical borehole on the right.

the source will remain trapped in this layer as a “guided” wave. The density ρ is constant everywhere. The layer contains 4000 cracks within an area of $800 \text{ m} \times 300 \text{ m}$, centered at $(500, 1500)$. For the two coordinates of each crack, a number is generated from a uniform distribution between 0 and 1 and subsequently scaled to the proper dimensions of the model. All the cracks have the same half-width $a_m = 1 \text{ m}$. We consider four cases:

the case without cracks, and cases with horizontally, vertically, and randomly oriented cracks. To generate the incident field, a point source is located in $(0, 1500)$. The source waveform is the Ricker wavelet (dominant frequency: 45 Hz). The total field at the receivers for the case of randomly oriented cracks is shown in Figure 6. Most energy of the wave field is trapped within the layer. Outside the layer, the wave field propagates faster and arrives earlier at the receivers.

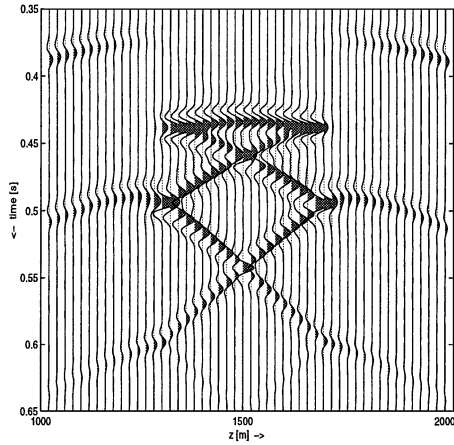


FIG. 6. Wave field transmitted through a low-velocity layer containing 4000 randomly oriented cracks. The geometry is shown in Figure 5. The wave field is clearly “trapped” in the layer.

Figure 7 shows the results for a receiver within the layer, located at $(1000, 1500)$, for all four cases. In Figure 7a, we can distinguish the different arrivals of the reflections. Figure 7b is a detail of Figure 7a. It clearly shows, that the signal for the case of horizontally oriented cracks coincides with the incident field until about $t = 0.44 \text{ s}$. Horizontally oriented cracks have hardly any effect on the wave field as long as it propagates parallel to the cracks. After reflection, the direction of the wave field has changed giving rise to more scattering by the horizontally oriented cracks. The cracks have the largest effect when oriented vertically; randomly oriented cracks have intermediate effects. Compared to the incident field, we observe two effects: the presence of the cracks affects the amplitudes and also results in a time delay.

DISCUSSION AND CONCLUSIONS

In this paper, we have presented a finite-difference method for computing the scattering of 2-D, scalar waves by many small-scale cracks, characterized by a Neumann boundary condition. This problem arises both in the scattering of *SH*-waves

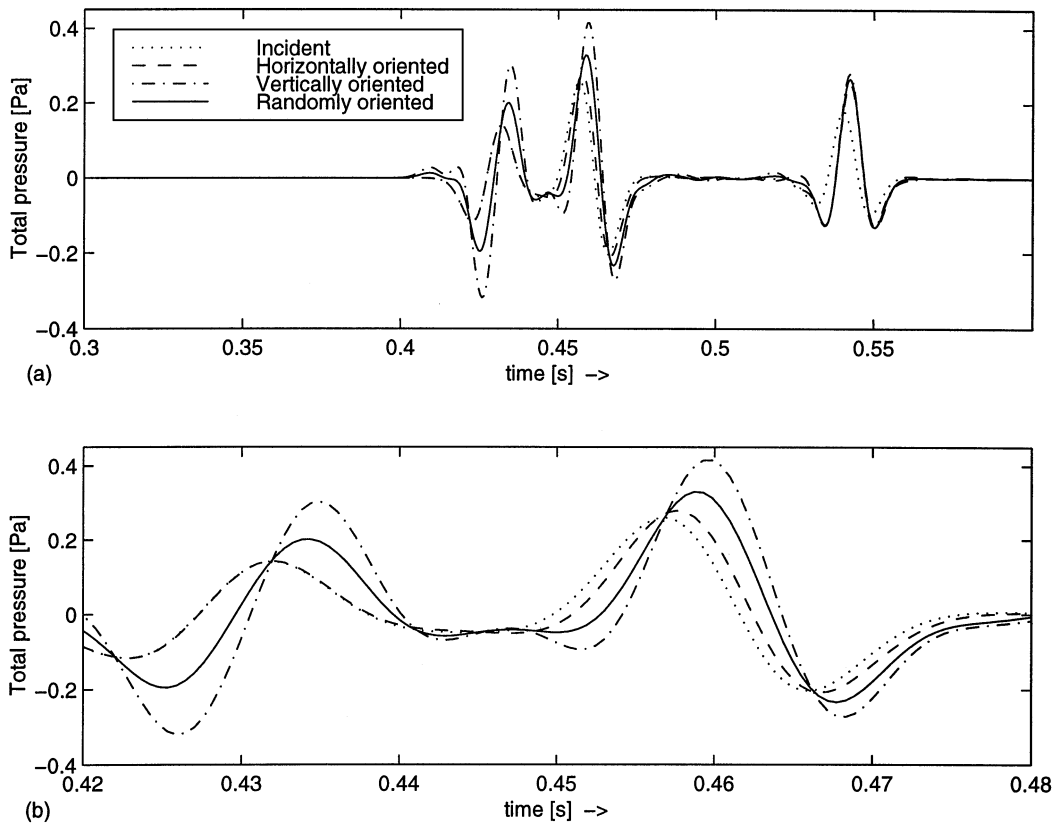


FIG. 7. Detailed comparison for a receiver at $(1000, 1500)$ for the case of Figure 5. Results are shown for the following cases: (1) no cracks (incident field only), (2) all cracks horizontally aligned, (3) all cracks vertically aligned, and (4) cracks randomly oriented. (a) Results between 0.3 and 0.6 s, (b) detail between 0.42 and 0.48 s.

in a solid containing stress-free cracks and in the scattering of pressure waves in a fluid medium containing rigid cracks. By considering only scalar problems, our paper addresses a simplified class of cracked media. As the cracks can be embedded in a heterogeneous medium, our method is an extension to methods based on integral equations which require a homogeneous background.

We have solved the problem of representing a small crack on a FD grid by deriving a suitable numerical source term. A further approximation of this source term provided a simpler expression that can be factored into a spatial and temporal part. This has resulted in a substantial reduction of computing time, without appreciable loss of accuracy, as became clear from the comparisons with the method of Mujres et al. (1998). For example, the CPU time required for running a simulation of 625 time steps for a grid of 62 500 points containing 3000 cracks on a single IBM/RISC System/6000 3AT is about 3 hours. The price paid for this efficiency is a restriction to first-order scattering. Although for the tested geometries, multiple scattering seemed to be negligible, it might still be important in other geometries. In attempting to include multiple scattering, we encountered severe accuracy problems. How to deal with multiple scattering between cracks in an efficient manner remains to be examined.

We have included some examples that illustrate the effect of cracks on the amplitude and phase of the incident field. The strength of these effects depends on the number, size, and orientation of the cracks.

The extension of the present method to three spatial dimensions is straightforward in principle, provided the relevant perturbation expression is used for computing the secondary source strength from the incident field. In the 3-D case, the approximation made to simplify the source term may not be necessary, because the 3-D Green's function does not involve a long history in time, as in the 2-D case.

To simplify the analytical representations, scalar wave propagation has been studied. In principle, also the full elastic problem can be treated in a similar way, although this extension is definitely not straightforward. It requires the asymptotic form of the elastic wavefield scattered by a small crack and the use of the elastic finite-difference operator to this field in order to find the appropriate distribution of the crack over the grid points. Recently, we have also solved the 2-D elastic case and will present the method in a forthcoming paper.

ACKNOWLEDGMENT

Helpful discussions of one of the authors (GCH) with Geza Seriani in an early stage of this project are gratefully acknowledged.

REFERENCES

- Abramowitz, M., and Stegun, I. A., 1972, Handbook of mathematical functions: Dover Publications.
- Burridge, R., and Chang, H. W., 1989, Multimode, one-dimensional wave propagation in a highly discontinuous medium: *Wave Motion*, **11**, 231–249.
- Carcione, J. M., 1996, Scattering of elastic waves by single anelastic cracks and fractures: 66th Ann. Internat. Mtg., Soc. Expl. Geophys., Expanded Abstracts, 654–657.
- Coates, R. T., and Schoenberg, M., 1995, Finite-difference modeling of faults and fractures: *Geophysics*, **60**, 1514–1526.
- Dablain, M. A., 1986, The application of higher-order differencing to the scalar wave equation: *Geophysics*, **51**, 54–66.
- De Hoop, A. T., 1955a, Variational formulation of two-dimensional diffraction problems with application to diffraction by a slit: *Proc. Kon. Ned. Akad. Wet.*, **B58**, 401–411.
- 1955b, On integrals occurring in the variational formulation of diffraction problems: *Proc. Kon. Ned. Akad. Wet.*, **B58**, 325–330.
- Hudson, J. A., and Knopoff, L., 1989, Predicting the overall properties of composite materials with small-scale inclusions or cracks: *Pageoph*, **131**, 551–576.
- Mujres, A. J. H., Herman, G. C., and Bussink, P. G. J., 1998, Acoustic wave propagation in two-dimensional media containing small-scale heterogeneities: *Wave Motion*, **27**, 137–154.
- O'Doherty, R. F., and Anstey, N. A., 1971, Reflections on amplitudes: *Geophys. Prosp.*, **19**, 430–458.

APPENDIX A

DISCRETE WAVE OPERATOR IN SPACE-FREQUENCY DOMAIN

With the scheme of Dablain (1986), the discrete wave operator is given by equation (19):

$$B^h p_{i,j}^n = \frac{p_{i,j}^{n+1} - 2p_{i,j}^n + p_{i,j}^{n-1}}{(c_{ij} \Delta t)^2} - \Delta^h p_{i,j}^n - \frac{(c_{ij} \Delta t)^2}{12} (\Delta^h)^2 p_{i,j}^n. \quad (\text{A-1})$$

To obtain its counterpart in space-frequency domain, we take the Fourier transform with respect to time. Furthermore, we use the relation

$$f(t - \Delta t) \xleftrightarrow{\mathcal{F}} e^{i\omega \Delta t} \hat{f}(\omega). \quad (\text{A-2})$$

For the finite-difference approximation of the second time derivative in equation (A-1), we then obtain

$$\frac{p_{i,j}^{n+1} - 2p_{i,j}^n + p_{i,j}^{n-1}}{(c_{ij} \Delta t)^2} \xleftrightarrow{\mathcal{F}} \frac{(e^{-i\omega \Delta t} - 2 + e^{i\omega \Delta t}) \hat{p}_{i,j}^n}{(c_{ij} \Delta t)^2}. \quad (\text{A-3})$$

The operator on the right side of this relation can be simplified to

$$\frac{(e^{i\omega \Delta t} - 2 + e^{-i\omega \Delta t})}{(c_{ij} \Delta t)^2} = \frac{-4 \sin^2 \left(\frac{\omega \Delta t}{2} \right)}{(c_{ij} \Delta t)^2}. \quad (\text{A-4})$$

If we apply a Taylor series expansion up to fourth order of the sine function, we obtain

$$\frac{-4 \sin^2 \left(\frac{\omega \Delta t}{2} \right)}{(c_{ij} \Delta t)^2} \cong -\frac{\omega^2}{c_{ij}^2} + \frac{1}{12} \frac{\omega^4}{c_{ij}^2} \Delta t^2 = -k_0^2 + \frac{(c_{ij} \Delta t)^2}{12} k_0^4. \quad (\text{A-5})$$

The spatial operator in equation (A-1) is not changed by the Fourier transformation and we arrive at equation (23):

$$\hat{B}^h = -k_0^2 + \frac{(\mu_{ij} \Delta s)^2}{12} k_0^4 - \left[\Delta^h + \frac{(\mu_{ij} \Delta s)^2}{12} (\Delta^h)^2 \right], \quad (\text{A-6})$$

where $c_{ij} \Delta t$ is replaced by $\mu_{ij} \Delta s$.

APPENDIX B

APPROXIMATION OF THE SOURCE DISTRIBUTION

To find a simple expression for the source distribution of a crack, the spatial part of relation equation (25) can be expanded using a Taylor series of the Hankel function $H_1^{(1)}(k_0 r_m)$.

Observing that

$$H_1^{(1)}(w) = J_1(w) - iY_1(w), \quad (\text{B-1})$$

and using the truncated Taylor series for the Bessel functions of first and second kind (Abramowitz and Stegun, 1972), we obtain

$$H_1^{(1)}(w) \cong \left\{ \frac{w}{2} - \frac{w^3}{16} \right\} - i \left\{ \frac{-2}{\pi w} + \left(\frac{-1 + 2\gamma_e - \log 4}{2\pi} \right) w \right. \\ \left. + \frac{w \log w}{\pi} + \left(\frac{5}{2} - 2\gamma_e + \log 4 \right) \frac{w^3 - \frac{w^3 \log w}{8\pi}}{16\pi} \right\}. \quad (\text{B-2})$$

Substitution of this expansion in equation (25), sorted into powers of k_0 and with $\xi_m = [\mathbf{n}_m \cdot (\mathbf{x} - \mathbf{x}_m)]$ the coordinate along the normal of the m th crack, yields

$$\hat{B}^h(\hat{p}_m^{sc}(\mathbf{x}, \omega)) = \pi a_m^2 \hat{q}_m(\omega) \left(-k_0^2 + \frac{(\mu_{ij} \Delta s)^2}{12} k_0^4 \right. \\ \left. - \left[\Delta^h + \frac{(\mu_{ij} \Delta s)^2}{12} (\Delta^h)^2 \right] \left(-\frac{\xi_m}{r_m(\mathbf{x})} k_0 \frac{i}{4} H_1^{(1)}(k_0 r_m) \right) \right) \\ \cong \pi a_m^2 \hat{q}_m(\omega) \left(\left[\Delta^h + \frac{(\mu_{ij} \Delta s)^2}{12} (\Delta^h)^2 \right] \frac{\xi_m}{2\pi r_m^2} \right. \\ \left. - k_0^2 \left\{ \frac{\xi_m}{2\pi r_m^2} + \left[\Delta^h + \frac{(\mu_{ij} \Delta s)^2}{12} (\Delta^h)^2 \right] \right\} \right. \\ \left. \times \frac{\xi_m}{8\pi} (1 - 2\gamma_e + \log 4) - \left[\Delta^h + \frac{(\mu_{ij} \Delta s)^2}{12} (\Delta^h)^2 \right] \right. \\ \left. \times \left(\frac{\xi_m \log k_0}{4\pi} + \frac{\xi_m \log r_m}{4\pi} - i \frac{\xi_m}{8} \right) \right\} \\ + k_0^4 \left\{ \frac{\mu_{ij} \Delta s}{12} - \frac{\xi_m}{8\pi} (1 - 2\gamma_e + \log 4) + \frac{\xi_m \log k_0}{4\pi} \right. \\ \left. + \frac{\xi_m \log r_m}{4\pi} + \left[\Delta^h + \frac{(\mu_{ij} \Delta s)^2}{12} (\Delta^h)^2 \right] \right\}$$

$$\times \left(\frac{\xi_m r_m^2}{64\pi} \left(\frac{5}{2} - 2\gamma_e + \log 4 \right) \right. \\ \left. - \frac{\xi_m r_m^2 \log k_0}{32\pi} - \frac{\xi_m r_m^2 \log r_m}{32\pi} \right) \\ + i \left(-\frac{\xi_m}{8} + \left[\Delta^h + \frac{(\mu_{ij} \Delta s)^2}{12} (\Delta^h)^2 \right] \frac{\xi_m r_m^2}{64} \right) \Bigg\}. \quad (\text{B-3})$$

If Δ^h is a n th-order operator, it can be shown that

$$\Delta^h \equiv \partial_{xx} + \partial_{zz} \quad (\text{B-4})$$

if applied to polynomials with degree less than or equal to n . For $n=4$, this leads to a considerable simplification in equation (B-3). Because

$$\Delta(\xi_m) = 0,$$

$$\Delta(\xi_m r_m^2) = 8\xi_m,$$

both the terms containing $\log k_0$ as well as the imaginary terms vanish and what remains is expression (26):

$$\hat{B}^h \hat{p}_m^{sc}(\mathbf{x}, \omega) \cong \pi a_m^2 [A_0(\mathbf{x}, \mathbf{x}_m) - k_0^2 A_2(\mathbf{x}, \mathbf{x}_m) \\ + k_0^4 A_4(\mathbf{x}, \mathbf{x}_m)] \hat{q}_m(\omega), \quad (\text{B-5})$$

with

$$A_0(\mathbf{x}, \mathbf{x}_m) = - \left[\Delta^h + \frac{(\mu_{ij} \Delta s)^2}{12} (\Delta^h)^2 \right] \frac{\mathbf{n}_m \cdot (\mathbf{x} - \mathbf{x}_m)}{2\pi r_m^2}, \quad (\text{B-6})$$

$$A_2(\mathbf{x}, \mathbf{x}_m) = \frac{\mathbf{n}_m \cdot (\mathbf{x} - \mathbf{x}_m)}{2\pi r_m^2} - \left[\Delta^h + \frac{(\mu_{ij} \Delta s)^2}{12} (\Delta^h)^2 \right] \\ \times \frac{\mathbf{n}_m \cdot (\mathbf{x} - \mathbf{x}_m) \log r_m}{4\pi}, \quad (\text{B-7})$$

$$A_4(\mathbf{x}, \mathbf{x}_m) = \frac{(\mu_{ij} \Delta s)^2 \mathbf{n}_m \cdot (\mathbf{x} - \mathbf{x}_m)}{12 \cdot 2\pi r_m^2} \\ + \frac{(3 + 4 \log r_m) \mathbf{n}_m \cdot (\mathbf{x} - \mathbf{x}_m)}{16\pi} - \left[\Delta^h + \frac{(\mu_{ij} \Delta s)^2}{12} (\Delta^h)^2 \right] \\ \times \frac{\mathbf{n}_m \cdot (\mathbf{x} - \mathbf{x}_m) r_m^2 \log r_m}{32\pi}, \quad (\text{B-8})$$

where ξ_m is replaced by $\mathbf{n}_m \cdot (\mathbf{x} - \mathbf{x}_m)$.